Improved solutions of the steady-state and the time-resolved diffusion equations for reflectance from a semi-infinite turbid medium

Alwin Kienle and Michael S. Patterson

Department of Medical Physics, Hamilton Regional Cancer Centre and McMaster University, 699 Concession Street, Hamilton, Ontario L8V 5C2, Canada

Received March 13, 1996; revised manuscript received August 20, 1996; accepted August 20, 1996

Improved solutions of the diffusion equation for time-resolved and steady-state spatially resolved reflectance are investigated for the determination of the optical coefficients of semi-infinite turbid media such as tissue. These solutions are derived for different boundary conditions at the turbid-medium–air interface and are compared with Monte Carlo simulations. Relative reflectance data are fitted in the time domain, whereas relative and absolute reflectance are investigated in the steady-state domain. It is shown that the error in deriving the optical coefficients is, especially for steady-state spatially resolved reflectance, considerably smaller for the solutions under study than for the commonly used solutions. Analysis of experimental measurements of absolute steady-state spatially resolved reflectance confirms these results. © 1997 Optical Society of America. [S0740-3232(97)03201-8]

1. INTRODUCTION

In recent years knowledge of photon migration in biological tissue has become an important tool for monitoring the physiological state of tissue.[1,2] Solutions of the diffusion equation have frequently been applied to derive the optical parameters from experimental data.[3–5] Although the diffusion equation is an approximation of the more exact transport equation,[6] it has the advantage that its solutions can be obtained in analytical form for relevant geometries.[7] However, for each solution the range of applicability has to be carefully examined. For example, Hielscher *et al.*[8] showed for time-resolved reflectance from a semi-infinite medium that the reduced scattering coefficient derived from solutions of the diffusion equation is incorrect if the source–detector distance is small. They applied three commonly used boundary conditions: the partial-current boundary condition (PCBC), the zero-boundary condition (ZBC), and the extrapolated-boundary condition (EBC). For the case of steady-state spatially resolved reflectance from a semi-infinite medium we previously pointed out that an EBC solution leads to great errors in deriving the optical coefficients for mismatched-boundary conditions.[9]

In this study we show that solutions of the diffusion equation that use EBC's can be significantly improved for steady-state spatially resolved and time-resolved reflectance from a semi-infinite medium by application of an approach used by Haskell *et al.*[10] for applications in the frequency domain. They calculated the reflectance from the integral of the reflected radiance and not from the gradient of the fluence rate. We investigated the errors in determining the reduced scattering μ_s' and the absorption coefficient μ_a by fitting the diffusion solutions to Monte Carlo simulations for time-resolved and spatially resolved reflectance. In the time domain we used relative data, and in the steady-state domain we used absolute and relative data. Measurements of absolute spatially resolved reflectance were used to confirm the theoretical calculations.

2. THEORY

We describe different solutions of the diffusion equation for time-resolved and steady-state spatially resolved reflectance from a semi-infinite turbid medium. The ZBC, the EBC, and the PCBC were applied to solve the diffusion equation.

A. Zero- and Extrapolated-Boundary Conditions

The ZBC states that the fluence rate is zero on the surface of the turbid medium, whereas the EBC states that the fluence rate goes to zero some distance beyond the actual surface. Employing the ZBC and the EBC and the method of image sources to solve the diffusion equation for the fluence rate Φ within the medium leads to[11,12]

$$\Phi(\rho, z, t) = \frac{c}{(4\pi Dct)^{3/2}} \exp(-\mu_a ct) \times \left\{ \exp\left[-\frac{(z - z_0)^2 + \rho^2}{4Dct} \right] - \exp\left[-\frac{(z + z_0 + 2z_b)^2 + \rho^2}{4Dct} \right] \right\}, \quad (1)$$

where $D = 1/[3(\mu_a + \mu_s')]$ is the diffusion constant, c is the speed of light in the turbid medium, ρ is the radial distance from the source, and z is the distance normal to the boundary. The first term is due to a point source at $z_0 = (\mu_a + \mu_s')^{-1}$ that results from the perpendicularly incident collimated light, and the second is due to a negative image source at $-z_0 - 2z_b$. For the ZBC z_b is zero, whereas it is

0740-3232/97/010246-09$10.00

$$z_b = \frac{1 + R_{\text{eff}}}{1 - R_{\text{eff}}} 2D \tag{2}$$

for the EBC. R_{eff} represents the fraction of photons that is internally diffusely reflected at the boundary. R_{eff} was calculated according to Haskell *et al.*,[10] who found that $R_{\text{eff}} = 0.493$ for a refractive index n of 1.4, which is representative of measured tissue data.[13,14] A thorough discussion of the quantity z_b can be found in Ref. 15. In the steady-state case (indicated by the superscript s) the fluence rate is given by[16]

$$\Phi^s(\rho, z) = \frac{1}{4\pi D}\left(\frac{\exp\{-\mu_{\text{eff}}[(z - z_0)^2 + \rho^2]^{1/2}\}}{[(z - z_0)^2 + \rho^2]^{1/2}} - \frac{\exp\{-\mu_{\text{eff}}[(z + z_0 + 2z_b)^2 + \rho^2]^{1/2}\}}{[(z + z_0 + 2z_b)^2 + \rho^2]^{1/2}}\right), \tag{3}$$

where $\mu_{\text{eff}} = [3\mu_a(\mu_a + \mu_s')]^{1/2}$.

In previous studies by Moulton,[12] by Hielscher *et al.*[8] and by others, the diffuse reflectance from the medium was calculated as the current across the boundary, with

$$R_f(\rho, t) = -D\nabla\Phi(\rho, z, t) \cdot (-\mathbf{z})\big|_{z=0}. \tag{4}$$

[If the reflectance is calculated with Eq. (4) we use the subscript f.] Inserting Eq. (1) into Eq. (4) yields

$$R_f(\rho, t) = \tfrac{1}{2}(4\pi Dc)^{-3/2} t^{-5/2} \exp(-\mu_a ct) \times \left[z_0 \exp\left(-\frac{{r_1}^2}{4Dct}\right) + (z_0 + 2z_b) \times \exp\left(-\frac{{r_2}^2}{4Dct}\right)\right], \tag{5}$$

where ${r_1}^2 = {z_0}^2 + \rho^2$ and ${r_2}^2 = (z_0 + 2z_b)^2 + \rho^2$. With Eqs. (3) and (4) the steady-state reflectance becomes

$$R_f{}^s(\rho) = \frac{1}{4\pi}\left[z_0\left(\mu_{\text{eff}} + \frac{1}{r_1}\right)\frac{\exp(-\mu_{\text{eff}} r_1)}{{r_1}^2} + (z_0 + 2z_b)\left(\mu_{\text{eff}} + \frac{1}{r_2}\right)\frac{\exp(-\mu_{\text{eff}} r_2)}{{r_2}^2}\right]. \tag{6}$$

As pointed out by Haskell *et al.*[10] it is more nearly correct to express the reflectance as the integral of the radiance over the backward hemisphere. In diffusion theory the radiance is expressed as the sum of two terms one proportional to the fluence rate and one proportional to the current or flux, which should be much smaller than the fluence rate term. The integral for the time-resolved or the steady-state reflectance can be written as[10]

$$R^{(s)}(\rho, t) = \int_{2\pi} \mathrm{d}\Omega[1 - R_{\text{fres}}(\theta)]\frac{1}{4\pi}\left[\Phi^{(s)}(\rho, z = 0, t) + 3D\frac{\partial\Phi^{(s)}(\rho, z = 0, t)}{\partial z}\cos\theta\right]\cos\theta, \tag{7}$$

where $R_{\text{fres}}(\theta)$ is the Fresnel reflection coefficient for a photon with an incident angle θ relative to the normal to the boundary. For a refractive index $n = 1.4$, Eq. (7) gives[10]

$$R^{(s)}(\rho, t) = 0.118\Phi^{(s)}(\rho, z = 0, t) + 0.306R_f{}^{(s)}(\rho, t). \tag{8}$$

We refer to Eq. (8) as the reflectance derived from the EBC, whereas if only the flux term is considered [Eq. (5) for the time domain and Eq. (6) for the steady-state domain] we use the abbreviation EBCF. For the ZBC the fluence rate is by definition zero at the physical boundary; therefore Eq. (5) with $z_b = 0$ is applied for time-resolved reflectance.

B. Partial-Current-Boundary Condition

In the partial-current-boundary treatment the irradiance at the boundary is set equal to the integral of the reflected radiance.[17] The solution for the time-resolved fluence rate in the medium when the PCBC is used is[10,18]

$$\Phi(\rho, z, t) = \frac{c}{(4\pi Dct)^{3/2}}\exp(-\mu_a ct) \times \left\{\exp\left[-\frac{(z - z_0)^2 + \rho^2}{4Dct}\right] + \exp\left[-\frac{(z + z_0)^2 + \rho^2}{4Dct}\right] - \frac{2}{z_b}\int_0^\infty \mathrm{d}l\, \exp(-l/z_b) \times \exp\left[-\frac{(z + z_0 + l)^2 + \rho^2}{4Dct}\right]\right\}, \tag{9}$$

and, employing the same method of images that was used to derive Eq. (9), we have for the steady-state fluence rate

$$\Phi^s(\rho, z) = \frac{1}{4\pi D}\left(\frac{\exp\{-\mu_{\text{eff}}[(z - z_0)^2 + \rho^2]^{1/2}\}}{[(z - z_0)^2 + \rho^2]^{1/2}} + \frac{\exp\{-\mu_{\text{eff}}[(z + z_0)^2 + \rho^2]^{1/2}\}}{[(z + z_0)^2 + \rho^2]^{1/2}} - \frac{2}{z_b}\int_0^\infty \mathrm{d}l\, \exp(-l/z_b) \times \frac{\exp\{-\mu_{\text{eff}}[(z + z_0 + l)^2 + \rho^2]^{1/2}\}}{[(z + z_0 + l)^2 + \rho^2]^{1/2}}\right). \tag{10}$$

Considering the radiance terms proportional to the flux and the fluence rate [Eq. (7)], we obtain for $n = 1.4$ for the time-resolved or steady-state reflectance[10]

$$R^{(s)}(\rho, t) = 0.170\Phi^{(s)}(\rho, z = 0, t). \tag{11}$$

Inserting Eq. (9) [Eq. (10)] into Eq. (11), one obtains the time-resolved (steady-state) reflectance for the PCBC.

We note that in the case of the PCBC the reflectance has also been derived from Eq. (4).[8,12] Hielscher *et al.*[8] showed that the results from this solution are similar to those from the EBCF solution. Thus it is not considered here.

C. Monte Carlo Simulations

In Sections 3 and 4 the solutions of the diffusion equations are compared with Monte Carlo simulations. The principles of Monte Carlo simulation of photon transport have been thoroughly described,[19,20] so we point out only the salient features of our self-written Monte Carlo program. A pencil photon beam was normally incident upon the semi-infinite turbid medium. The Henyey–Greenstein[21] phase function was assumed for calculation of the scattering angle. For the Monte Carlo simulations in the time domain a spatial resolution of 0.5 mm and a temporal resolution of 2.5 ps for $t < 100$ ps and of 10 ps for $t > 100$ ps were chosen for scoring the reflectance. The simulations were run for a certain reduced scattering coefficient and for zero absorption. From these data we calculated the reflectance curves with different absorption coefficients, using Beer's law and the path length of the photons through the turbid medium.[22] This approach has the advantages that only one simulation is needed for reflectance curves with different absorption coefficients and that the statistic of the reflectance at long times is improved. The anisotropy factor g was chosen to be 0.8, because g values between 0.8 and 1 do not influence the reflectance significantly as long as μ_s' is constant.[23]

The spatial resolution of the steady-state Monte Carlo simulations was 0.1 mm, and distances up to 25 mm were scored. For the anisotropy factor 0.9 was chosen. As in the time domain, the steady-state spatially resolved reflectance is practically invariant if $g \geqslant 0.8$ and μ_s' is constant.[9]

For the nonlinear regression a combination of the gradient search method and the method of linearizing the fitting function was used.[24] The logarithm of the reflectance data was fitted in nonlinear regressions for investigations both in the time domain and in the steady-state domain. Equal weights for all the data points were used in the fitting procedure. The logarithm of the reflectance using equal weights was employed because it was more robust than other possibilities (e.g., fitting the raw reflectance data with equal weights or with weights calculated from $1/R$). Also, the optical properties could be found most accurately in this way.

3. TIME-DOMAIN REFLECTANCE

A. Comparison with Monte Carlo Simulations

Figures 1 and 2 compare time-resolved reflectance from a semi-infinite turbid medium calculated with the solutions for the EBC with only the flux term and with both the flux and the fluence terms with Monte Carlo simulations at two distances, 4.75 and 9.75 mm, and for three distances, 4.75, 9.75, and 14.75 mm. In Fig. 1 the PCBC solution is also shown. The optical coefficients for the curves shown in Fig. 1 are $\mu_a = 0.02$ mm^{-1} and $\mu_s' = 1$ mm^{-1}, and those for the curves in Fig. 2 are $\mu_a = 0.02$ mm^{-1} and $\mu_s' = 0.5$ mm^{-1}. Using the diffusion solution that includes the flux and the fluence terms [Eq. (8)] results in an improvement at early times compared with the solution of Eq. (5), for which only the flux term is considered. At longer times the different solutions are close to the Monte Carlo simulation (and also close to experiments[25]). The deviation from the Monte Carlo simulation occurs at approximately 100–200 ps, whereas for the EBCF solution it occurs at approximately 200–400 ps. For the PCBC solution the deviation occurs between those of the other two solutions. Thus the PCBC solution is worse than the EBC solution, although its boundary condition is physically more rigorous. The reasons for this are unclear.

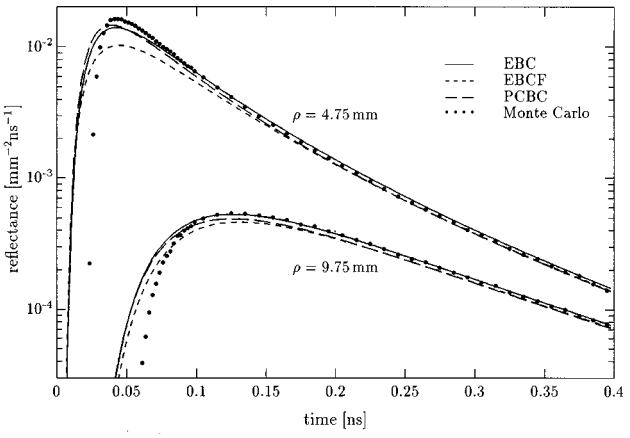

Fig. 1. Comparison of time-resolved diffuse reflectance, calculated by means of diffusion theory with different boundary conditions, with Monte Carlo simulations at $\rho = 4.75$, 9.75 mm. The optical coefficients are $\mu_s' = 1$ mm^{-1}, $\mu_a = 0.02$ mm^{-1}, $g = 0.8$, and $n = 1.4$.

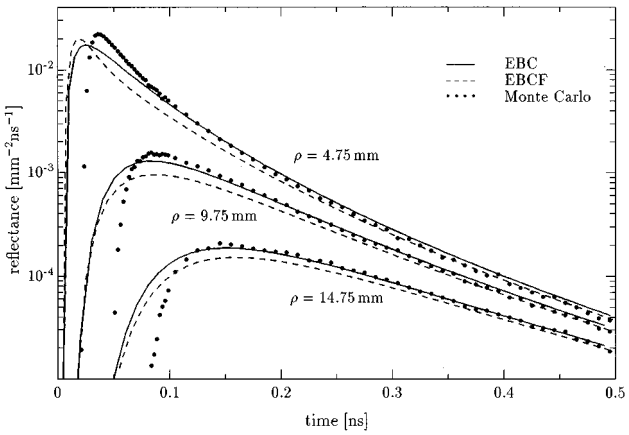

Fig. 2. Comparison of time-resolved diffuse reflectance, calculated by means of diffusion theory with different boundary conditions, with Monte Carlo simulations at $\rho = 4.75$, 9.75, and 14.75 mm. The optical coefficients are $\mu_s' = 0.5$ mm^{-1}, $\mu_a = 0.02$ mm^{-1}, $g = 0.8$, and $n = 1.4$.

B. Derivation of the Optical Coefficients

To investigate how the different solutions of the diffusion equation influence the derivation of the optical properties from time-resolved reflectance measurements, we fitted the corresponding equations to Monte Carlo simulations. Because relative measurements were assumed, three parameters were fitted: μ_s', μ_a, and a multiplicative factor. This is similar to the approach taken by Hielscher *et al.*,[8] but we used the improved solutions for the EBC and the PCBC.

Figures 3 and 4 show the derived reduced scattering and absorption coefficients, respectively, for a nonlinear regression to a Monte Carlo simulation calculated for $\mu_s' = 1\ \text{mm}^{-1}$, $\mu_a = 0.02\ \text{mm}^{-1}$ and $\rho = 9.75$ mm. The optical coefficients are plotted versus the time at which the first reflectance value was used for the nonlinear regression. This start time was gradually increased to demonstrate the influence of the reflectance at early times where diffusion theory is least accurate. The data were fitted up to times at which the reflectance is greater than 10^{-4} times the maximum value of the reflectance, because this dynamic range is the best that can be achieved for typical time-domain reflectance measurements.[8]

As Fig. 3 indicates, the accuracy with which μ_s' can be determined depends on which diffusion solution is used. Disregarding the reflectance data at times earlier than 100 ps, the errors in μ_s' for the different models are

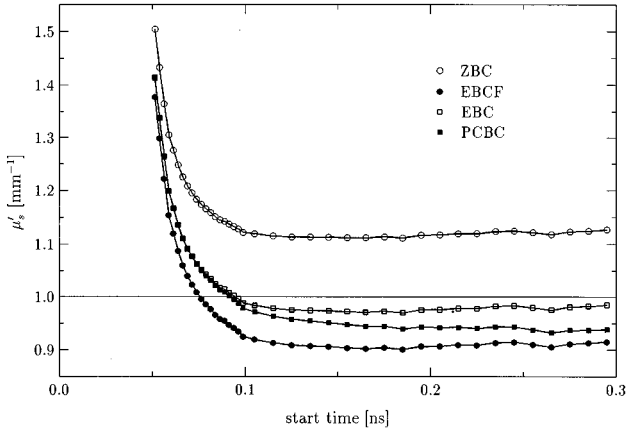

Fig. 3. Reduced scattering coefficients derived from nonlinear regressions of different solutions of the diffusion equation for time-resolved reflectance to a Monte Carlo simulation versus the start time of the fitting range. The optical coefficients of the Monte Carlo simulation are $\mu_s' = 1\ \text{mm}^{-1}$, $\mu_a = 0.02\ \text{mm}^{-1}$, and $n = 1.4$, and the distance from the source is $\rho = 9.75$ mm.

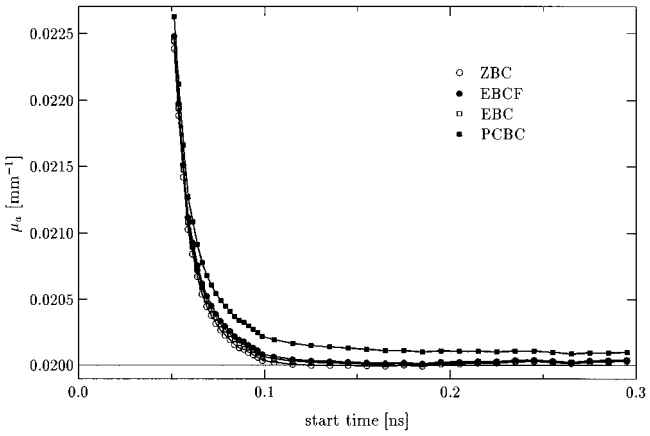

Fig. 4. Absorption coefficients derived from nonlinear regressions of different solutions of the diffusion equation for time-resolved reflectance to a Monte Carlo simulation versus the start time of the fitting range. The optical coefficients of the Monte Carlo simulation are $\mu_s' = 1\ \text{mm}^{-1}$, $\mu_a = 0.02\ \text{mm}^{-1}$, and $n = 1.4$, and the distance from the source is $\rho = 9.75$ mm.

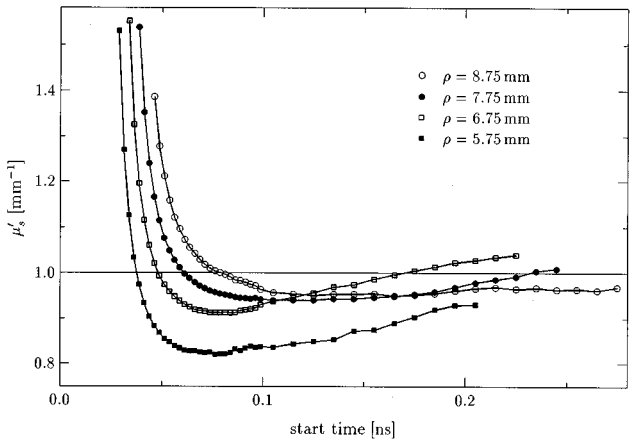

Fig. 5. Reduced scattering coefficients derived from nonlinear regressions of the EBC solution for time-resolved reflectance to Monte Carlo simulations with different $\mu_s'\rho$ values versus the start time of the fitting range. The optical coefficients of the Monte Carlo simulation are $\mu_s' = 1\ \text{mm}^{-1}$, $\mu_a = 0.02\ \text{mm}^{-1}$, and $n = 1.4$ and the distances from the source, ρ, are shown.

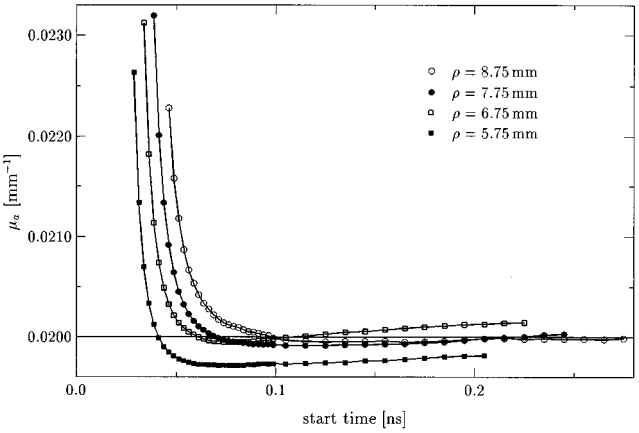

Fig. 6. Absorption coefficients derived from nonlinear regressions of the EBC solution for time-resolved reflectance to Monte Carlo simulations with different $\mu_s'\rho$ values versus the start time of the fitting range. The optical coefficients of the Monte Carlo simulation are $\mu_s' = 1\ \text{mm}^{-1}$, $\mu_a = 0.02\ \text{mm}^{-1}$, and $n = 1.4$, and the distances from the source, ρ, are shown.

~12% for the ZBC, ~9% for the EBCF, ~6% for the PCBC, and ~2% for the EBC, whereas the error in μ_a is always smaller than 1% for this fitting region regardless of which model is used. Additional nonlinear regressions for other distances and optical coefficients revealed that, although the EBC solution is closest to the Monte Carlo simulation, the derived optical coefficients were not always better than those derived with the other solutions. This is because relative data were fitted, and thus the shape of the curves is more important than the absolute values. This is especially true if early times are not included in the calculations.

In general, diffusion theory is valid if the photons have experienced many scattering interactions, i.e., $\mu_s'\rho \gg 1$. In the example above this product is $\mu_s'\rho = 9.75$. For

greater values the errors in the optical properties derived with the same fitting approach as in Figs. 3 and 4 decrease, whereas they increase for smaller values. To examine this effect quantitatively we fitted the EBC solution to Monte Carlo data for different $\mu_s'\rho$. Figures 5 and 6 show the derived reduced scattering and absorption coefficients, respectively. We altered the product $\mu_s'\rho$ by changing the source–detector distance, 5.75 mm $\leqslant \rho \leqslant$ 8.75 mm, whereas the reduced scattering coefficient was held constant, $\mu_s' = 1\ \text{mm}^{-1}$. The absorption coefficient was $\mu_a = 0.02\ \text{mm}^{-1}$.

Figure 5 indicates that the error in determining μ_s' exceeds 10% for distances smaller than ~7 mm ($\mu_s'\rho < 7$) if the data at the early times are disregarded. Similar calculations for $\mu_s' = 0.5\ \text{mm}^{-1}$ and $\mu_s' = 1.5\ \text{mm}^{-1}$ showed also that the error in deriving the reduced scattering exceeds 10% for $\mu_s'\rho < 7$. The absorption coefficient (see Fig. 6) can be derived within 2%.

We note that the derivation of the optical coefficients from the diffusion solutions also depends on the absorption coefficient. In general, it can be stated that the errors in determining μ_s' decrease if the absorption coefficient is decreased, and vice versa.

4. STEADY-STATE REFLECTANCE

A. Comparison with Monte Carlo Simulations

Figure 7 compares the steady-state spatially resolved reflectance with the EBC solution and with the EBCF solution to a Monte Carlo simulation. The optical coefficients are $\mu_s' = 1\ \text{mm}^{-1}$, $\mu_a = 0.01\ \text{mm}^{-1}$, and in the Monte Carlo simulations the anisotropy factor is $g = 0.9$. Figure 7 shows that the EBC solution approximates the Monte Carlo simulations much better than does the EBCF solution. Only for distances smaller than 1.5 mm are systematic differences greater than 5% seen, whereas for the EBCF solution this is the case for distances up to 10 mm. Figure 8 compares these curves for a smaller distance range, and, in addition, the PCBC solution is shown. This solution is worse than the EBC solution for distances smaller than 4 mm. Therefore in Subsections 4.B and 4.C the EBC solution is applied.

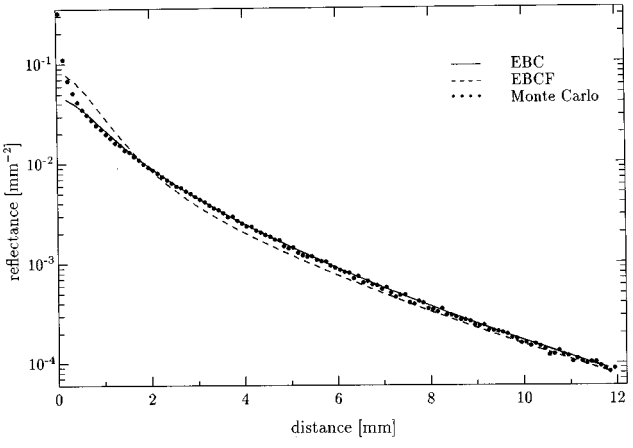

Fig. 7. Comparison of steady-state spatially resolved reflectance, calculated by means of diffusion theory with different boundary conditions (EBCF and EBC), with Monte Carlo simulations. The optical coefficients are $\mu_s' = 1\ \text{mm}^{-1}$, $\mu_a = 0.01\ \text{mm}^{-1}$, $g = 0.9$, and $n = 1.4$.

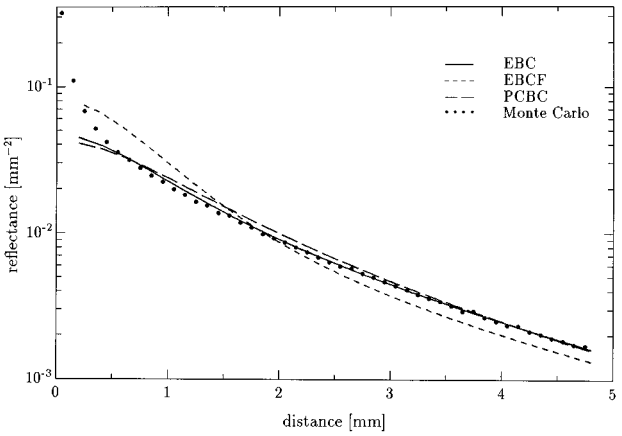

Fig. 8. Comparison of steady-state spatially resolved reflectance, calculated by means of diffusion theory with different boundary conditions (EBCF, EBC, and PBCC), with Monte Carlo simulations. The distance range is decreased compared with that shown in Fig. 7. The optical coefficients are $\mu_s' = 1\ \text{mm}^{-1}$, $\mu_a = 0.01\ \text{mm}^{-1}$, $g = 0.9$, and $n = 1.4$.

B. Derivation of the Optical Coefficients from Absolute Steady-State Spatially Resolved Reflectance

Here the errors in deriving the optical properties from absolute steady-state spatially resolved reflectance are investigated. Recently we showed that it is possible to measure absolute spatially resolved reflectance with a CCD camera.[9] There it was also pointed out that the application of the EBCF solution often results in errors of ~50% or ~100%.

Because of the absolute reflectance data, only two parameters, μ_s' and μ_a, were fitted. The EBC solution was used in the nonlinear regression to reflectance data generated with the Monte Carlo method for different distance ranges. Figures 9 and 10 show contour plots of the absolute values of the relative error in deriving μ_s' and μ_a, respectively, versus the start and the end distances of the fitting range. The start distance is varied from 0.35 to 4.05 mm in steps of 0.1 mm; the end distance, from 5.95 to 24.95 mm in steps of 1 mm. The optical coefficients of the Monte Carlo simulations are $\mu_s' = 1\ \text{mm}^{-1}$, $\mu_a = 0.01\ \text{mm}^{-1}$, $g = 0.9$, and $n = 1.4$.

Figure 9 shows that the error in deriving μ_s' is less than 6% for start distances up to almost 4 mm. The errors in deriving μ_a are smaller than 15% for the entire fitting range and are mostly smaller than 10%; see Fig. 10. The random errors caused by statistical uncertainty in the Monte Carlo data are in the range of a few percent and have no influence on the general conclusions. We performed calculations similar to those of Figs. 9 and 10 for $\mu_s' = 1\ \text{mm}^{-1}$ and different absorption coefficients ($\mu_a = 0.003,\ 0.005,\ 0.03,\ 0.05\ \text{mm}^{-1}$). In the range of the investigated absorption coefficients the relative errors in the derived optical coefficients decreased if the absorption coefficient was increased, and vice versa. For example, for $\mu_a = 0.003\ \text{mm}^{-1}$ the maximum error in the derived absorption coefficient was ~25% and in the reduced scattering coefficient it was ~10% for start distances smaller than 3 mm. The reason for this is prob-

ably that a certain relative change of the absorption coefficient alters the spatially resolved reflectance more when μ_a is great compared with the case in which μ_a is small. Therefore a certain relative difference between the diffusion equation and Monte Carlo data results in a greater error of the derived optical properties if μ_a is small. In contrast, even for $\mu_a = 0.05\ \mathrm{mm}^{-1}$ the reduced scattering coefficient is 20 times greater than the absorption coefficient. Thus the diffusion approximation is still valid. We note that the results of these contour plots calculated for $\mu_s' = 1\ \mathrm{mm}^{-1}$ can be used for other reduced scattering coefficients, because it is possible to scale the data. For example, the error contour plots in Figs. 9 and 10 are the same for $\mu_s' = 0.5\ \mathrm{mm}^{-1}$ and $\mu_a = 0.005\ \mathrm{mm}^{-1}$ if the start and the end distances are multiplied by two.

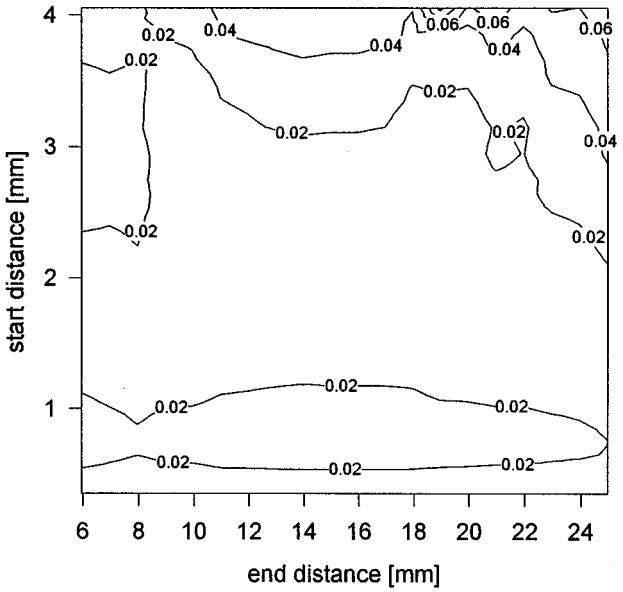

Fig. 9. Absolute values of the relative errors of the reduced scattering coefficients derived from nonlinear regressions of the steady-state EBC solution to Monte Carlo data of absolute spatially resolved reflectance. The start and the end distances of the fitting range are varied. The optical coefficients of the Monte Carlo simulations are $\mu_s' = 1\ \mathrm{mm}^{-1}$, $\mu_a = 0.01\ \mathrm{mm}^{-1}$, $g = 0.9$, and $n = 1.4$.

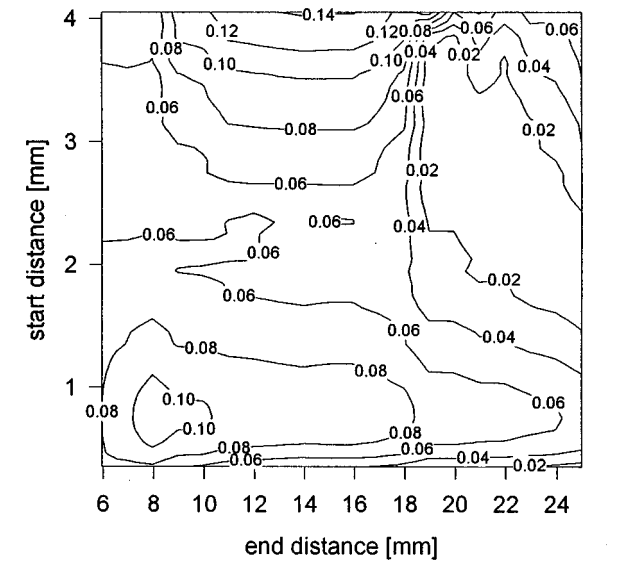

Fig. 10. Absolute values of the relative errors of the absorption coefficients derived from nonlinear regressions of the steady-state EBC solution to Monte Carlo data of absolute spatially resolved reflectance. The start and the end distances of the fitting range are varied. The optical coefficients of the Monte Carlo simulations are $\mu_s' = 1\ \mathrm{mm}^{-1}$, $\mu_a = 0.01\ \mathrm{mm}^{-1}$, $g = 0.9$, and $n = 1.4$.

C. Derivation of the Optical Coefficients from Relative Steady-State Spatially Resolved Reflectance

Most of the experimental data presented in the literature are based on relative steady-state spatially resolved reflectance measurements. Because of the lack of the absolute values and the need to fit an additional parameter, the ability of the nonlinear regression algorithm to recover the correct optical coefficients is worse than the fit of absolute reflectance data.

Figures 11 and 12 show contour plots of the absolute values of the relative errors in deriving μ_s' and μ_a, respectively, versus the start and the end distances of the fitting range. The optical coefficients and the fitting range are the same as in Figs. 9 and 10.

These figures show that, in general, the errors are greater than the nonlinear regression to the absolute reflectance. For the derivation of μ_s' the errors are as much as ~20% for small end distances, but they are smaller than 10% if the end distance is greater than 12 mm. The errors of the derived absorption coefficients are greater than those for the reduced scattering coefficients, especially at small end distances of the fitting range; see Fig. 12. For end distances greater than ~12 mm the errors are smaller than 20%. Calculations similar to those shown in Figs. 11 and 12 were performed for $\mu_s' = 1\ \mathrm{mm}^{-1}$ and $\mu_a = 0.003$, 0.005, 0.03, 0.05 mm^{-1}. In general, they showed the same behavior with respect to start and end distances, although the errors were somewhat greater. However, for start distances smaller than 2 mm and end distances greater than 15 mm the errors were smaller than 25% in deriving μ_a and smaller than 15% in deriving μ_s'. Once again, these results can be transferred to other reduced scattering coefficients by scaling. For example, for $\mu_s' = 0.5\ \mathrm{mm}^{-1}$ the errors in deriving μ_s' are smaller than 15% if the start distance is smaller than 4 mm and the end distance is greater than 30 mm.

D. Absolute Steady-State Spatially Resolved Reflectance Measurements

We made absolute steady-state spatially resolved reflectance measurements, using a CCD camera. These measurements were described in detail previously.[9] Briefly, a He–Ne laser at $\lambda = 633$ nm with a beam diameter of 0.4 mm was incident approximately perpendicularly upon a tissue phantom, which consisted of diluted Intralipid as

the scattering medium and Trypan Blue as the absorbing medium. The diffusely reflected photons were imaged onto a CCD camera, and the intensity values were recorded. From these records the spatially resolved reflectance was calculated. Absolute measurements were possible because we also recorded the incident beam with the CCD camera by replacing the phantom with a mirror. The true optical coefficients of the phantom were derived from the independently measured reduced scattering coefficient of Intralipid and the absorption coefficient of Trypan Blue. Table 1 shows the reduced scattering and absorption coefficients derived from a nonlinear regression with the EBC solution and the EBCF solution of four measurements of the absolute spatially resolved reflectance. The true optical coefficients are also given in the table. A distance range of 2–12 mm was used for the nonlinear regression.

Table 1 indicates that with the diffusion solution consisting only of the EBCF it is not possible to derive the optical coefficients accurately. For two measurements no result could be obtained because the nonlinear regression diverged. With the EBC solution, however, the optical coefficients can be derived quite satisfactorily. The errors are smaller than 10%, except for the phantom with the lowest absorption coefficient. This behavior of the nonlinear regression to absolute spatially resolved reflectance data was described in Subsection 4.B and probably occurs because even a large fractional change in μ_a will have little effect on the reflectance curve if μ_a is small.

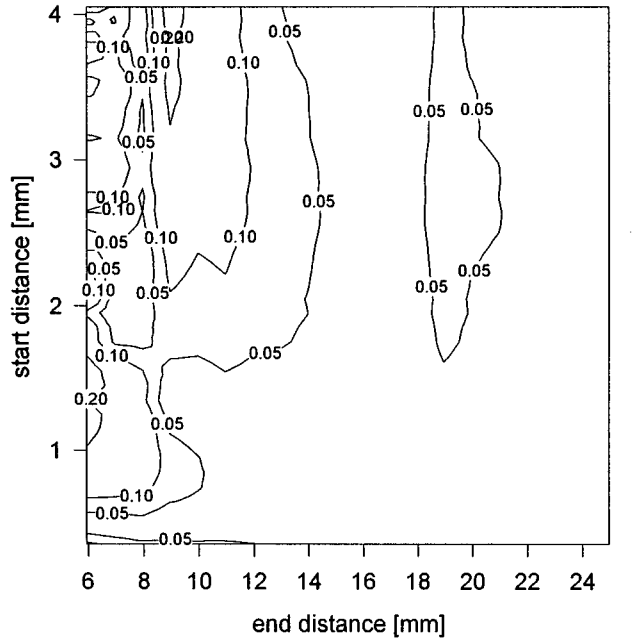

Fig. 11. Absolute values of the relative errors of the reduced scattering coefficients derived from nonlinear regressions of the steady-state EBC solution to Monte Carlo data of relative spatially resolved reflectance. The start and the end distances of the fitting range are varied. The optical coefficients of the Monte Carlo simulations are $\mu_s' = 1\ \text{mm}^{-1}$, $\mu_a = 0.01\ \text{mm}^{-1}$, $g = 0.9$, and $n = 1.4$.

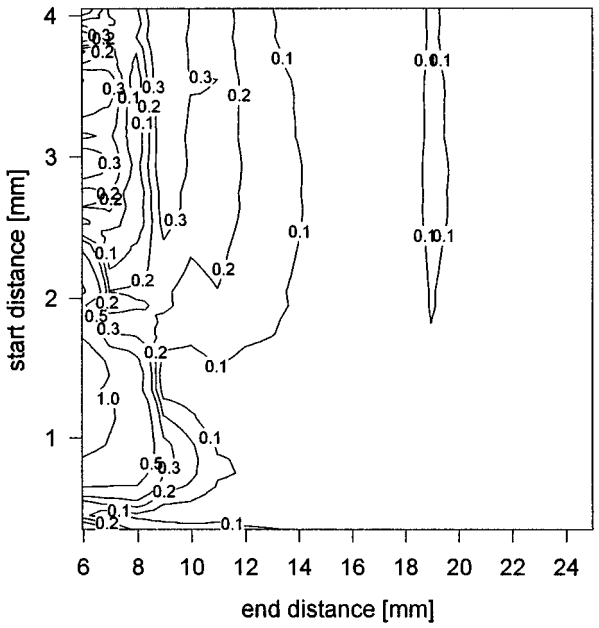

Fig. 12. Absolute values of the relative errors of the absorption coefficients derived from nonlinear regressions of the steady state EBC solution to Monte Carlo data of relative spatially resolved reflectance. The start and the end distances of the fitting range are varied. The optical coefficients of the Monte Carlo simulations are $\mu_s' = 1\ \text{mm}^{-1}$, $\mu_a = 0.01\ \text{mm}^{-1}$, $g = 0.9$, and $n = 1.4$.

5. DISCUSSION AND CONCLUSIONS

We applied improved solutions of the diffusion equation for time-resolved and steady-state spatially resolved reflectance from a semi-infinite medium as originally used by Haskell *et al.*[10] in the frequency domain. In contrast

Table 1. Optical Properties Derived from Nonlinear Regressions to Spatially Resolved Absolute Reflectance Measurements on Phantoms by Use of the EBC Solution [Eq. (8)] and the EBCF Solution [Eq. (6)][a]

True Optical Properties (mm^{-1})		EBC Solution (mm^{-1})		EBCF Solution (mm^{-1})	
μ_a	μ_s'	μ_a	μ_s'	μ_a	μ_s'
0.0033	0.98	0.0024	1.11	Divergent	Divergent
0.0088	0.98	0.0080	1.07	Divergent	Divergent
0.025	0.97	0.026	1.02	0.013	1.53
0.070	0.94	0.074	0.91	0.051	1.27

[a] For comparison the true optical coefficients are also shown.

to their results, we found a significant improvement when we used the flux and the fluence terms to calculate the reflectance.

In the time domain we showed that the new equations describe the reflectance correctly for times approximately twice as short as for the previously used equations. In general, this method of calculation results in smaller errors in deriving the optical coefficients from the time-resolved reflectance. However, because relative data were used in the nonlinear regression, this is not always the case, especially when the fitting range includes only the decreasing part of the reflectance curve.

For steady-state spatially resolved reflectance it was pointed out that the new equation that we obtained by applying the EBC results in a great improvement compared with results from previously used equations. Significant deviations from Monte Carlo simulations occur only at distances smaller than $\sim 1.5/\mu_s'$, whereas this critical distance is more than five times greater for the EBCF solution.

When the EBC solution was used to fit absolute spatially resolved reflectance data generated with Monte Carlo simulations it was shown that the errors in deriving μ_s' and μ_a were smaller than 10% and 15%, respectively, for practically relevant distance ranges. For nonlinear regressions to relative spatially resolved reflectance data the errors are in general greater and depend more on the distance range used for the fit. Therefore, one must consider the possible range of the optical coefficients of the investigated samples and the distance range of the measurements to decide whether the optical parameters can be derived with the needed accuracy.

For applications for which the errors from the improved EBC solution are too great, a neural network trained with Monte Carlo data can be used for both the steady state[9,26] and the time-resolved reflectances. One can obtain even more-accurate results by fitting the output of one Monte Carlo simulation to the experimental data by applying Beer's law and scaling techniques.[23]

For the calculations of the reflectance in Eq. (7) it was assumed that all remitted photons are detected independently of the emission angle. To investigate the effect of detectors that have a small numerical aperture and that are oriented normal to the boundary of the turbid medium, we calculated the steady-state reflectance for these conditions [using the approximation $\cos(\theta) \approx 1$ in Eq. (7)] and compared it with the results computed with Eq. (7). We found that the differences were small except for small distances to the source. For example, for $\mu_s' = 1$ mm^{-1} and $\mu_a = 0.01$ mm^{-1} the difference between the two curves is smaller than 5% for all the distances greater than 1.3 mm. In a recent study similar results were found with the Monte Carlo method.[9]

Finally, we compared the EBCF solution and the EBC solution of the diffusion equation by analyzing experimental absolute spatially resolved reflectance measurements. With the new solution (EBC) it was possible to deduce the optical coefficients of the measured tissue phantoms mostly within errors of 10%, whereas with the old solution EBCF it was not possible to derive the correct coefficients.

ACKNOWLEDGMENTS

This study was supported by National Institutes of Health grant PO1-CA43892. A. Kienle is grateful for a postdoctoral scholarship from the German Research Society (Deutsche Forschungsgemeinschaft).

REFERENCE

1. J. P. Vanhouton, D. A. Benaron, S. Spilman, and D. K. Stevenson, "Imaging brain injuries using time-resolved near-infrared light scanning," Pediatr. Res. 39, 470–476 (1996).
2. A. Knüttel, S. Koch, R. Schork, and D. Böcker, "Tissue characterization with optical coherence tomography (OCT)," *Biomedical Sensing, Imaging, and Tracking Technologies I*, R. A. Lieberman, H. Podbielska, and T. V. O-Dinh, eds., Proc. SPIE **2676**, 54–64 (1996).
3. S. Fantini, M. A. Franceschini, S. Fishkin, B. Barbieri, and E. Gratton, "Quantitative determination of the absorption spectra of chromophores in strongly scattering media: a light-emitting-diode-based technique," Appl. Opt. **33**, 5204–5213 (1994).
4. B. W. Pogue and M. S. Patterson, "Frequency-domain optical absorption spectroscopy of finite tissue volumes using diffusion theory," Phys. Med. Biol. **39**, 1157–1180 (1994).
5. H. Liu, A. Hielscher, B. Chance, S. L. Jacques, and F. K. Tittel, "Influence of blood vessels on the measurement of hemoglobin oxygenation as determined by time-resolved reflectance spectroscopy," Med. Phys. **22**, 1209–1217 (1995).
6. A. Ishimaru, *Wave Propagation and Scattering in Random Media* (Academic, New York, 1978), Chaps. 7 and 9.
7. S. R. Arridge, M. Cope, and D. T. Delpy, "The theoretical basis for the determination of optical pathlengths in tissue: temporal and frequency analysis," Phys. Med. Biol. **37**, 1531–1560 (1992).
8. A. H. Hielscher, S. L. Jacques, L. Wang, and F. K. Tittel, "The influence of boundary conditions on the accuracy of diffusion theory in time-resolved reflectance spectroscopy of biological tissue," Phys. Med. Biol. **40**, 1957–1975 (1995).
9. A. Kienle, L. Lilge, M. S. Patterson, R. Hibst, R. Steiner, and B. C. Wilson, "Spatially resolved absolute diffuse reflectance measurements for noninvasive determination of the optical scattering and absorption coefficients of biological tissue," Appl. Opt. **35**, 2304–2314 (1996).
10. R. C. Haskell, L. O. Svaasand, T. T. Tsay, T. C. Feng, M. McAdams, and B. J. Tromberg, "Boundary conditions for the diffusion equation in radiative transfer," J. Opt. Soc. Am. A **11**, 2727–2741 (1994).
11. M. S. Patterson, B. Chance, and B. C. Wilson, "Time resolved reflectance and transmittance for the noninvasive measurement of tissue optical properties," Appl. Opt. **28**, 2331–2336 (1989).
12. J. D. Moulton, "Diffusion modelling of picosecond laser pulse propagation of turbid media," master's degree dissertation (McMaster University, Hamilton, Ontario, Canada, 1990).
13. F. P. Bolin, L. E. Preuss, R. C. Taylor, and R. J. Ference, "Refractive index of some mammalian tissue using a fiber optic cladding method," Appl. Opt. **28**, 2297–2303 (1989).
14. G. J. Tearney, M. E. Brezinski, J. F. Southern, B. E. Bouma, M. R. Hee, and J. G. Fujimoto, "Determination of the refractive index of highly scattering human tissue by optical coherence tomography," Opt. Lett. **20**, 2258–2260 (1995).
15. R. Aronson, "Boundary conditions for diffusion of light," J. Opt. Soc. Am. A **12**, 2532–2539 (1995).
16. T. J. Farrell, M. S. Patterson, and B. C. Wilson, "A diffusion theory model of spatially-resolved, steady-state diffuse reflectance for the noninvasive determination of tissue optical properties *in vivo*," Med. Phys. **19**, 879–888 (1992).
17. M. Keijzer, W. M. Star, and P. R. M. Storchi, "Optical diffusion in layered media," Appl. Opt. **27**, 1820–1824 (1988).
18. G. H. Bryan, "An application of the method of images to the

conduction of heat," Proc. London Math. Soc. **22**, 424–430 (1891).
19. B. C. Wilson and G. Adam, "A Monte Carlo model for the absorption and flux distribution of light in tissue," Med. Phys. **10**, 824–830 (1983).
20. L. Wang, S. L. Jacques, and L. Zheng, "MCML—Monte Carlo modeling of light transport in multi-layered tissues," Comput. Methods Programs Biomed. **47**, 131–146 (1995).
21. L. G. Henyey and J. L. Greenstein, "Diffuse radiation in galaxy," Astrophys. J. **93**, 70–83 (1941).
22. R. Graaff, M. H. Koelink, F. F. M. de Mul, W. G. Zijlstr, A. C. M. Dassel, and J. G. Aarnoudse, "Condensed Monte Carlo simulations for the description of light transport," Appl. Opt. **32**, 426–434 (1993).
23. A. Kienle and M. S. Patterson, "Determination of the optical properties of turbid media from a single Monte Carlo simulation," Phys. Med. Biol. **41**, 2221–2227 (1996).
24. P. R. Bevington, *Data Reduction and Error Analysis for the Physical Sciences* (McGraw-Hill, New York, 1983), Chap. 11.
25. F. Liu, K. M. Yoo, and R. R. Alfano, "Should the photon flux of the photon density be used to describe the temporal profiles of scattered ultrashort laser pulses in random media?" Opt. Lett. **18**, 432–434 (1993).
26. T. J. Farrell, B. C. Wilson, and M. S. Patterson, "The use of a neural network to determine tissue optical properties from spatially resolved diffuse reflectance measurements," Phys. Med. Biol. **37**, 2281–2286 (1992).